

## Neutron Diffraction Studies of CO<sub>2</sub> Clathrate Hydrate: Formation from Deuterated Ice

Robert W. Henning,<sup>†</sup> Arthur J. Schultz,<sup>\*,†</sup> Vu Thieu,<sup>‡</sup> and Yuval Halpern<sup>\*,‡</sup>

*Intense Pulsed Neutron Source, Argonne National Laboratory, Argonne, Illinois 60439, and Energy Systems Division, Argonne National Laboratory, Argonne, Illinois 60439*

*Received: January 12, 2000; In Final Form: March 28, 2000*

The formation of CO<sub>2</sub> clathrate hydrate was investigated by using time-of-flight neutron powder diffraction at temperatures ranging from 230 to 290 K with a CO<sub>2</sub> gas pressure of 900 psi. CO<sub>2</sub> clathrate hydrate was prepared in situ from deuterated ice crystals at 230, 243, 253, and 263 K by pressurizing the system with CO<sub>2</sub> gas to produce the hydrate in approximately 70% yield. Nearly complete conversion from the hexagonal ice to the sI type CO<sub>2</sub> hydrate was observed as the temperature of the sample was slowly increased through the melting point of D<sub>2</sub>O ice. The conversion of ice into hydrate is believed to be a two-stage process in which an initial fast conversion rate is followed by a slower, diffusion-limited rate. On the basis of a shrinking core diffusion model, an activation energy of 6.5 kcal/mol was obtained from the temperature dependence of the reaction. Our findings suggest that the formation of the hydrate is through a reaction between CO<sub>2</sub> and water molecules in the quasi-liquid layer (QLL). The CO<sub>2</sub> hydrate remained stable following removal of excess liquid CO<sub>2</sub> and subsequent pressurization with helium, allowing for a low-temperature (14 K) structure analysis from powder diffraction data without the presence of solid CO<sub>2</sub>.

### Introduction

Clathrate hydrates (commonly called gas hydrates) are solid inclusion compounds in which water forms cagelike structures around smaller guest molecules. Hydrate formation takes place when water molecules come into contact with gas molecules (such as methane, propane, and carbon dioxide) at high pressures and low temperatures. Details about gas hydrates and their properties are reviewed in a recent monograph.<sup>1</sup> Gas hydrates represent a source of problems for the natural gas and oil industries because hydrate formation often causes blockages in production pipelines.<sup>2</sup> On the other hand, large deposits of gas hydrates found around the U.S. continental margin represent an enormous supply of reserve energy, if the gas (primarily methane) could be recovered safely and economically.<sup>3</sup> Environmental concerns over the increase of carbon dioxide in the environment and global warming have prompted investigations into ways of storing carbon dioxide for extended periods. This could be achieved by sequestration of the excess carbon dioxide within a hydrate framework.<sup>4–6</sup>

The crystalline structures of hydrates have been determined, under equilibrium conditions, by means of X-ray and NMR techniques.<sup>7–10</sup> Studies of the formation and dissociation processes of hydrates, on the other hand, typically involve measurements of temperature and pressure changes of the gas and liquid phases to infer the properties and rate of structural changes of the hydrate phase. Recent experiments employing Raman spectroscopy have provided insight into the mechanism of hydrate formation, as well as the development of kinetics models.<sup>11,12</sup> These kinetics models naturally will be essential in assessing such issues as the feasibility of producing gas from clathrate hydrates and controlling formation rates in sequestering excess carbon dioxide as hydrate clathrate.

The use of powder X-ray diffraction for studies of carbon dioxide, propane, and methane hydrates has been reported.<sup>13–15</sup> Although neutron diffraction has been used to study methane, nitrogen, and oxygen hydrates,<sup>15–17</sup> only two recent papers are available on a neutron diffraction study of carbon dioxide clathrate.<sup>18,19</sup> In those experiments, the samples were prepared over periods of several months in the laboratory prior to the neutron data collection. However, we have focused on measuring time-dependent formation processes of the carbon dioxide hydrate starting from ice. This publication describes the first observation by neutron diffraction of the in situ formation processes of carbon dioxide hydrates. These experiments were carried out using the high-intensity powder diffractometer (HIPD) instrument at the Intense Pulsed Neutron Source (IPNS) at Argonne National Laboratory.

### Experimental Section

**Apparatus.** A high-pressure sample cell intended for pressures up to 15 000 psi (100 MPa) and for temperatures at room temperature or below was designed and fabricated at Argonne National Laboratory (Figure 1). The main part of the cell is aluminum alloy (7075-T6) with a wall thickness of  $1/16$  in. and an inside diameter of  $5/16$  in. The top part of the cell is brass and is mounted to the aluminum base with 10 brass screws, with a lead gasket between the two pieces. CO<sub>2</sub> (99.9%) from a standard gas cylinder is introduced into the system through a stainless steel line that connects to the side of the brass top. A cadmium shield was mounted around the base of the pressure cell to minimize neutron diffraction peaks from the aluminum container.

**Sample Preparation.** Powdered ice was obtained by freezing deuterated water (Aldrich, 99.9%) in liquid nitrogen and then crushing the ice in a mortar and pestle. Large ice particles were removed with a 250  $\mu$ m sieve, and the powdered ice was placed in the pressure cell that was already cooled in liquid nitrogen. The pressure cell was closed, mounted on the cold stage of a

\* To whom correspondence should be addressed.

<sup>†</sup> Intense Pulsed Neutron Source, Argonne National Laboratory.

<sup>‡</sup> Energy Systems Division, Argonne National Laboratory.

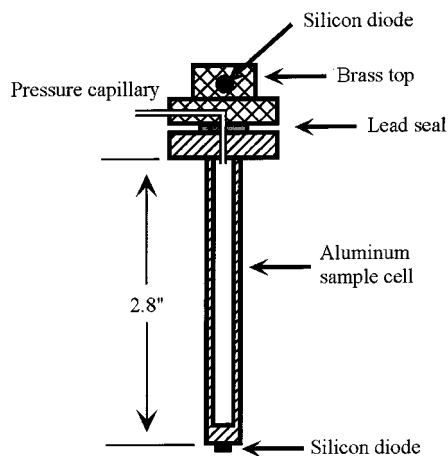


**Figure 1.** Schematic drawing of the aluminum pressure cell with silicon diode temperature sensors.

Displex closed-cycle helium refrigerator, and put into the sample chamber on the HIPD diffractometer. The pressure cell was kept in liquid nitrogen throughout this process to prevent the ice from melting and to discourage condensation buildup on the outside of the cell. This is a concern because the incoherent scattering of the hydrogen would cause a high background in the data collection. Before the CO<sub>2</sub> gas was introduced into the system, the ice was allowed to stabilize at the desired temperature. The CO<sub>2</sub> gas was introduced rapidly with a pressure of ~900 psi. A temperature increase of ~5 K was observed but returned to the starting temperature within a few minutes. This is believed to be due to the rapid formation of the CO<sub>2</sub> hydrate, which is an exothermic reaction, and the condensation of the pressurizing gas that was at room temperature.

**Data Analysis.** Data were collected in 15 min intervals starting with the initial introduction of the gas into the system. The total length of the data collection depended on the initial starting temperature with longer times required at lower temperatures. Time-of-flight powder diffraction data were obtained by using the 90° data bank on the HIPD, which is conceptually similar to the GPPD and SEPD instruments at IPNS<sup>20</sup> but with a short initial flight path (moderator-to-sample) of 5.5 m and a secondary flight path (sample-to-detectors) of 1 m. This gives a higher incident neutron flux at the expense of resolution with respect to the other diffractometers. Data were analyzed using the GSAS program.<sup>21</sup>

The short data collection times and relatively low resolution of the HIPD instrument did not allow for a full Rietveld analysis of each data set. The lattice parameters of the three phases observed in the spectrum—CO<sub>2</sub> hydrate, ice, and aluminum—were refined in the initial stages but then fixed because the temperature and pressure of the sample did not change. The atomic positions and thermal parameters were determined in separate experiments for each temperature and were not allowed to change during the refinements. Besides the four background parameters, only the histogram scale factor, an absorption coefficient, and the phase fractions were allowed to refine. The weight fractions were extracted from each refinement, adjusted for the gain of CO<sub>2</sub> in the solid phase, and plotted in terms of mole fractions of hydrate.

**Structure.** The sample was prepared as described above at 263 K and 900 psi and ramped in temperature to 278 K to obtain 98% conversion. Excess CO<sub>2</sub> was removed by first stabilizing the sample at 263 K and then releasing the CO<sub>2</sub> pressure to 1 atm by opening a valve used to isolate the sample from the atmosphere. This valve was kept open for several minutes to

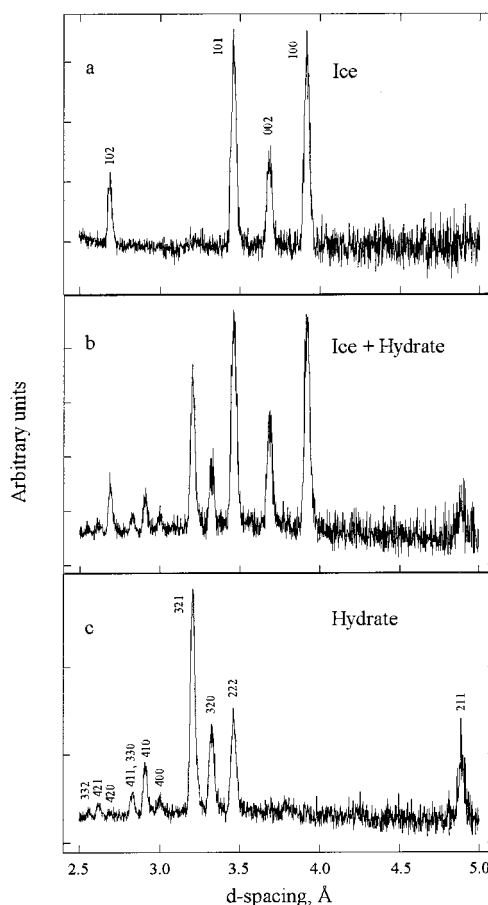


**Figure 2.** Transformation of D<sub>2</sub>O ice to CO<sub>2</sub> hydrate: (a) ice at 263 K before adding CO<sub>2</sub>; (b) mixture of ice and CO<sub>2</sub> hydrate at 263 K and 900 psi; (c) CO<sub>2</sub> hydrate at 276.4 K and 900 psi. The noisy background is due to the short collecting times of 15 min per histogram.

vent all of the CO<sub>2</sub> gas. Complete gas removal was confirmed by closing the valve and noting that the cell pressure stabilized around 1 atm. The sample was then repressurized with 2200 psi of helium. Additional confirmation for the complete removal of excess CO<sub>2</sub> was provided by the absence of solid CO<sub>2</sub> diffraction peaks when this sample was brought down to 14 K for structural analysis.

The data collection was performed on the general purpose powder diffractometer (GPPD) at 14 K.<sup>20</sup> Data were obtained from both 90° banks and combined into one histogram for the final Rietveld refinement. The preferred orientation in the aluminum peaks was accounted for by using the March–Dollase routines in GSAS.

## Results and Discussion

Neutron diffraction is a useful tool to follow the structural changes that occur as the sample changes under different conditions. Neutrons are strongly penetrating, which allows for the use of high-pressure equipment and cryogenic devices with relative ease. If a full structural refinement is performed, neutron diffraction also locates the hydrogen atom positions with much higher precision than can be obtained by X-ray diffraction studies.

**Formation.** CO<sub>2</sub> hydrates typically form around 273 K (0 °C) and under moderate pressure.<sup>22,23</sup> Diffraction data from a typical formation experiment are shown in Figure 2. The sample of D<sub>2</sub>O ice was stabilized at 263 K (−10 °C), and before the sample was pressurized with CO<sub>2</sub>, data were collected to confirm that ice could be observed in the powder pattern (Figure 2a).

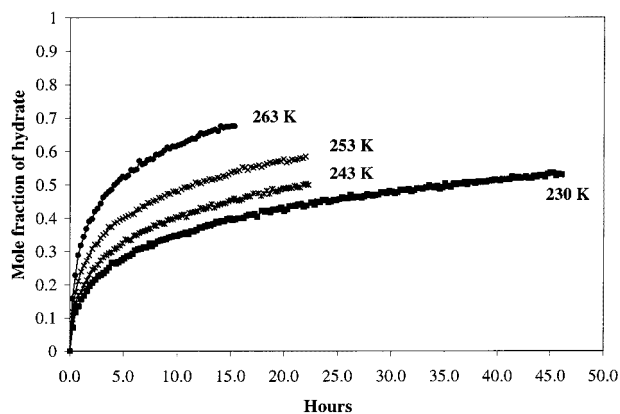


**Figure 3.** Conversion of deuterated ice to carbon dioxide hydrate at  $\sim 900$  psi at various temperatures. Each data point represents the mole fraction of hydrate refined from a 15 min histogram.

Hexagonal ice was clearly present as well as some peaks from the aluminum pressure cell. The aluminum lines occur at a  $d$  spacing of 2.34 Å and below, so they are not observed in the plots in Figure 2. The structural parameters obtained from a Rietveld refinement of the ice sample were consistent with previous reports and did not reveal any preferred orientation, suggesting that the sample did not melt during the preparation.

When the sample was pressurized to  $\sim 900$  psi (6.2 MPa) with  $\text{CO}_2$ , the temperature increased by  $\sim 5$  K but the system equilibrated within 5 min. Given the temperature and pressure,  $\text{CO}_2$  should have condensed inside the pressure cell. Figure 2b shows that at an intermediate point in the experiment the peaks corresponding to the sI-type  $\text{CO}_2$  hydrate<sup>7</sup> formed. From Rietveld refinements of each of these 15 min time slices, the mole fraction of hydrate is shown to increase with time (Figure 3). This plot also shows similar results for experiments performed at 230, 243, and 253 K. The conversion of ice to hydrate is a temperature-dependent process with  $\sim 50\%$  conversion occurring in 35, 22, 12, and 4 h at 230, 243, 253, and 263 K, respectively. Repeated experiments at 230 and 243 K indicated a reproducibility of  $\pm 5\%$  in the determination of mole fractions vs time. In addition to all the other experimental factors, this also indicates that the grain size distribution is quite reproducible. The reduced reaction rate and limited instrument time prevented a complete conversion to the hydrate under these conditions, with  $\sim 50$ – $70\%$  conversion normally observed.

Complete conversion to the hydrate ( $\sim 98\%$ ) was obtained by keeping the sample pressurized with  $\text{CO}_2$  and slowly warming it through the melting point of  $\text{D}_2\text{O}$  ice, which is 276.8 K (3.8 °C). The sample was heated from 272.2 to 278.0 K in steps of 0.2 K every 15 min. Data were collected during each of these 15 min intervals to observe the transformation. Very little change was observed until the sample reached 275.6 K at the top of the cell. The peaks corresponding to ice slowly disappeared, while the hydrate peaks increased in intensity. The diffraction peaks corresponding to the ice disappeared completely at a temperature of 276.4 K (Figure 2c). The lower melting point is consistent with the system being under pressure. Even though the amount of hydrate increased as the ice decreased, it is possible that some of the remaining ice simply melted and did not form the hydrate. This was confirmed by cooling the sample back to 263 K and observing small peaks corresponding to  $\sim 2\%$  ice. Attempts to convert the remaining ice to hydrate by either keeping the system under a pressure of  $\text{CO}_2$  for longer time periods ( $\sim 12$  h) or by ramping the temperature more slowly did not succeed. Similar results were reported by Stern et al.<sup>24</sup>

From observations of the formation of  $\text{CH}_4$  and  $\text{CO}_2$  hydrates from ice under similar conditions (200  $\mu\text{m}$  grain size and  $\sim 900$  psi for  $\text{CO}_2$  and up to 4400 psi for  $\text{CH}_4$ ), a “superheating” effect of the ice above the normal melting point has been suggested.<sup>14,24,25</sup> This was inferred from the lack of a significant pressure decrease in the methane system as the melting point of ice was reached. Independent pressure–temperature measurements were not performed in the carbon dioxide system, but optical experiments suggested that the superheating effect may also occur in this system. Our current data on the  $\text{CO}_2$  hydrate clearly show that the ice remaining in the granular cores does not persist above the normal melting point of  $\text{D}_2\text{O}$  under these conditions.

**Kinetics.** Although changes in the shape and texture of the particles could not be determined from our experiments, direct observation of  $\text{CO}_2$  hydrate formation on the surface of ice grains has been previously reported by Stern et al.<sup>25</sup> In those experiments, the surface of the ice became mottled as the hydrate formed but no fracturing of the particles was observed. We believe that after an initial period of fast conversion on the surface of the ice particles, the process is controlled by the diffusion rate of  $\text{CO}_2$  molecules through the accumulating hydrate layer. This has also been suggested by Hwang et al.<sup>26</sup> and Stern et al.,<sup>24</sup> but no quantitative measurements have been reported. The following equation describes a conversion process of a particle from the outside during its diffusion-controlled stage at a constant temperature:<sup>27</sup>

$$(1 - \alpha)^{1/3} = \left( \frac{-(2k)^{1/2}}{r_0} \right) (t - t^*)^{1/2} + (1 - \alpha^*)^{1/3} \quad (1)$$

where  $k$  and  $r_0$  are the diffusion constant and the original radius of the particles, and  $\alpha$  and  $\alpha^*$  are degrees of reactions at times  $t$  and  $t^*$ . This equation has recently been used to fit the shrinking core model of the hydration of cement grains<sup>28,29</sup> and should also be applicable to the inward growth of a hydrate layer on an ice particle. For each temperature, obtaining a straight line by plotting  $(1 - \alpha)^{1/3}$  as a function of  $(t - t^*)^{1/2}$  indicates an agreement with eq 1. For a given particle size, the diffusion constant ( $k$ ) can be calculated from the slope of the straight line. Since the fine fraction was not removed with a sieve, an accurate quantitative determination of the diffusion constants cannot be obtained with the current data. However, with reproducible grain size distributions, accurate temperature dependencies and activation energies are obtained (vide infra).

The term  $t^*$  indicates the time where the conversion process is initially dominated by the diffusion of  $\text{CO}_2$  molecules through the hydrate layer. In our experiments, we selected the  $t^*$  corresponding to  $\sim 20\%$  conversion for each of the temperatures. This produced the best linear fit of eq 1 to the data. Plots in which  $t^*$  did not correspond to 20% conversion deviated from the linear line. For low values of  $(t - t^*)^{1/2}$ , the slope increases for  $t^*$  corresponding to  $< 20\%$  conversion and decreases for  $t^*$  corresponding to  $> 20\%$  conversion, indicating that diffusion became the dominant factor in the reaction rate at  $t^*$  corresponding to  $\sim 20\%$  conversion. Figure 4 shows a plot of our data in terms of eq 1 for each of the four temperatures.

The diffusion constants depend on the particle size and temperature, but for a given particle size distribution ( $r_0$ ), the activation energy of the diffusion process is independent of these variables. The temperature dependence of a thermally dependent diffusion process should follow Arrhenius behavior described by  $k = A \exp[-E_a/(RT)]$ , where  $R$  is the gas constant. If we define  $k/r_0^2$  as  $k'$ , we can calculate  $k'$  for each temperature from

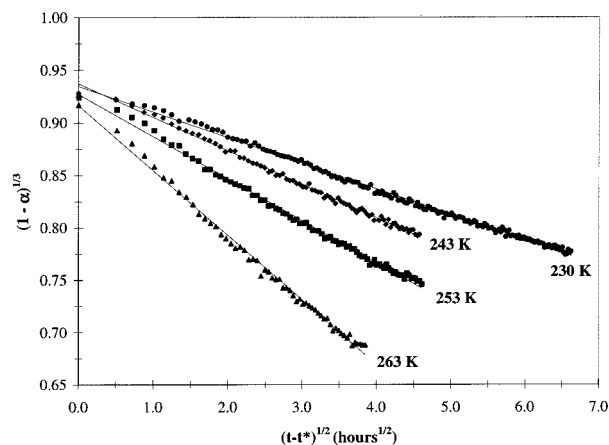


**Figure 4.** Plot of experimental data in terms of eq 1 at four different temperatures.

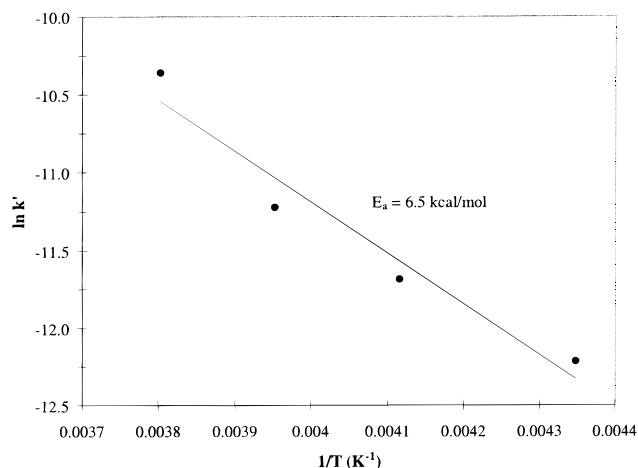


**Figure 5.** Plot of  $\ln(k')$  as a function of  $1/T$  ( $K^{-1}$ ). An activation energy of the diffusion process was calculated from the slope of the straight line.

the slopes in Figure 4. Figure 5 shows the straight line obtained by plotting  $\ln(k')$  against  $1/T$ . An activation energy value of 6.5 kcal/mol was calculated from the slope of this line.

The value of 23.5 kJ/mol (5.6 kcal/mol) for the activation energy for diffusion by the translational motion of H<sub>2</sub>O molecules in the quasi-liquid layer (QLL) has been reported.<sup>30</sup> This value is in good agreement with the value of approximately 5 kcal/mol for the hydrogen bond energy in water.<sup>1</sup> Even though we have employed D<sub>2</sub>O rather than H<sub>2</sub>O in our study, we feel it is justified to compare our results to those obtained for H<sub>2</sub>O systems because the difference in hydrogen bonding energy between hydrogen and deuterium is less than 1 kJ/mol (0.24 kcal/mol).<sup>31</sup> Our finding indicates that after approximately 20% conversion the rate-limiting step of the process is the diffusion of CO<sub>2</sub> molecules through the layer of hydrate. This is in agreement with the suggestion that the slower growth rate of CO<sub>2</sub> hydrates in a water drop covered with a thin film of CO<sub>2</sub> hydrate may be caused by the slow transport of CO<sub>2</sub> molecules across the growing solid hydrate layer.<sup>32</sup> Furthermore, we suggest that after the diffusion through the hydrate layer the formation of the hydrate is through a reaction between CO<sub>2</sub> and water molecules in the QLL where the hydrogen bond energy is approximately 5 kcal/mol rather than a reaction between CO<sub>2</sub> and ice where the hydrogen bond energy is in excess of 0.55 eV (12.7 kcal/mol).<sup>33</sup> This is consistent with previous reports of a "premelting" layer where enhanced hydrate formation may occur at a liquidlike surface film on the ice grains.<sup>24,34</sup> Takeya

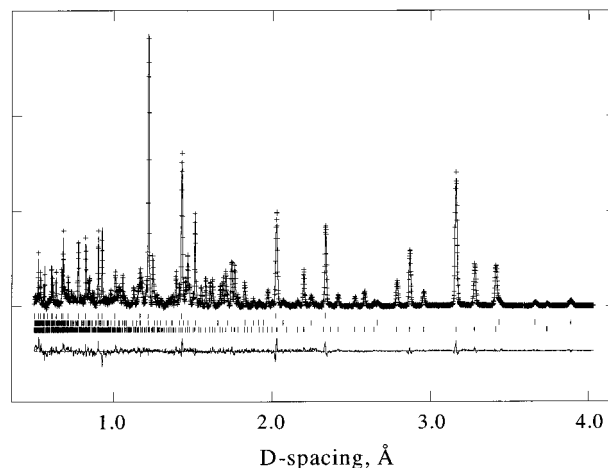


**Figure 6.** Neutron powder diffraction pattern of aluminum, hexagonal ice, and carbon dioxide hydrate. The tick marks below the histogram are in the same order as above. The difference between the observed and calculated pattern is printed on the bottom.

et al.<sup>35</sup> used X-ray diffraction to study the transformation of ice to CO<sub>2</sub> hydrate and reported the value of 0.2 eV (4.6 kcal/mol) for the activation energy of the initial reaction period. They suggest transformation of liquid water rather than ice as the mechanism of the initial reaction of converting ice into CO<sub>2</sub> hydrates.

Furukawa and Nada reported<sup>36</sup> that the thickness of the QLL depends strongly on the temperature. Their experimental results show 2 orders of magnitude decrease in QLL thickness by supercooling ice to a  $\Delta T$  of 10 K. The availability of internal liquid water in our experiments is probably a result of partial melting of ice in the interface due to evolution of heat of adsorption and heat of reaction. This explanation is in agreement with the report that the heat of adsorption together with the heat liberated in the process of capturing the guest molecule in the cage allows the evolution of restructured water molecules at the interface in a self-catalytic reaction.<sup>37</sup>

**Structure.** A low-temperature neutron powder data set was collected at  $\sim 14$  K and analyzed by standard Rietveld methods to examine the details of the interactions between the carbon dioxide molecules and the framework water molecules. A recent neutron diffraction study by Ikeda et al.<sup>18</sup> of the temperature dependence of the structure of the CO<sub>2</sub> hydrate concluded that the CO<sub>2</sub> molecules remain dynamically disordered below 100 K. This is consistent with the results of our experiment described below. Our analysis was complicated by the presence of two additional compounds; aluminum ( $\sim 66$  wt %, from the pressure cell) and ice ( $\sim 2$  wt %). Both of these extra phases have small unit cells and are well defined, but some overlap of the peaks still occurs, especially at small  $d$  spacings, which introduces some uncertainty in the hydrate structure. The difference between the observed and calculated data is displayed at the bottom of Figure 6 with the largest discrepancies occurring with some of the aluminum peaks.

An interesting aspect of our structural study was the fact that we could remove the excess liquid CO<sub>2</sub> at 263 K and pressurize the sample with 2200 psi of He without appreciable dissociation of the hydrate. This allowed for a simpler Rietveld refinement at 14 K because no solid CO<sub>2</sub> was present. Some dissociation of the hydrate (and a corresponding increase in the amount of ice) was expected to occur under these conditions, since CO<sub>2</sub> hydrate is not thermodynamically stable at 263 K and 1 atm,<sup>1</sup> but no change in the relative amounts of hydrate and ice was observed.



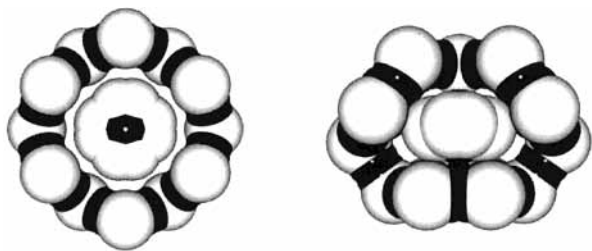


**Figure 7.** van der Waals surface plots of the disordered carbon dioxide molecule inside the large ( $5^{12}6^2$ ) cavity. The picture on the left is viewed down the  $4_2$  screw axis, and the right picture has the  $4_2$  screw axis vertical. Selected atoms were removed from the cage in order to view the guest molecule more clearly.

The  $D_2O$  framework is well defined and is consistent with previous reports about structure type I hydrates.<sup>7</sup> Hydrogen bonding interactions create a rigid framework with each oxygen atom fully occupied but tetrahedrally coordinated by four partially occupied deuterium atoms. All deuterium atoms display disorder between two sites with each site fixed at 50% occupancy. The carbon dioxide molecules reside in two types of voids, which are formed by the framework water molecules. The carbon dioxide molecules display strong disorder within each cavity and require a more detailed interpretation. All atomic positions and thermal parameters are well behaved and are listed in the Supporting Information.

The largest void is a tetrakaidecahedron ( $5^{12}6^2$ ) with the oxygen atoms forming 12 pentagonal and 2 hexagonal faces. The deuterium atoms are disordered between the oxygen positions. The ellipsoidal shape and size of the cavity is well suited for a carbon dioxide molecule. The distance across the waist of the cavity is  $\sim 6.2$  Å (after van der Waals interactions are accounted for), while the shorter dimension is  $\sim 3.2$  Å.<sup>1</sup> The linear  $CO_2$  molecule is  $\sim 5.12$  Å long, which gives plenty of room within the waist of the cavity but does not allow for much movement out of the plane (Figure 7). NMR measurements by Ratcliffe and Ripmeester suggest that the  $CO_2$  molecule can deviate up to  $31^\circ$  out of the equatorial plane.<sup>38</sup> Fourier neutron density maps show a large diffuse peak at the center of the cavity with additional density distributed  $\sim 1.1$  Å away from the central peak but confined to within the largest dimension of the cavity. This distance corresponds to the C–O distance in solid  $CO_2$ , so this has been interpreted as carbon at the center with the oxygen atoms disordered around it. Although the size and shape of the cavity appears to restrict the  $CO_2$  molecule to the largest dimensions of the cavity, the guest molecule does not appear to have any preferred orientation within this plane. The model that provided the best fit to the data was a  $CO_2$  molecule disordered over four sites with the carbon atom fixed at the center of the cavity. The refined C–O distance in the guest molecule was 1.18(3) Å, whereas the corresponding distance in solid  $CO_2$  is 1.121(3) Å.

Twelve oxygen atoms form the smaller void in a pentagonal dodecahedron arrangement ( $5^{12}$ ). The roughly spherical cavity is not ideal for a linear guest molecule but provides a tight fit for  $CO_2$ . The van der Waals diameter of the cavity is roughly equal to the length of the carbon dioxide molecule. Fourier nuclear density maps reveal the carbon atom at the center of the cavity as expected with the oxygen atoms disordered on a sphere  $\sim 1.1$  Å away. As with the other void, the carbon dioxide molecule was refined as disordered but over six different sites. The refined C–O distance was 1.166(9) Å.

The disorder of the guest molecules and the multiphase refinement made it difficult to determine the amount of  $CO_2$  in

the structure. A strong correlation between the occupancy of the carbon and oxygen atoms of the  $CO_2$  with their thermal parameters prevented a combined refinement. A large range of values have been reported in the literature with only the large cavity being occupied in a few cases<sup>38,39</sup> to both cages being occupied up to 90 and 98% for the small and large voids, respectively.<sup>18,19,22</sup> The difference in reported occupancies is consistent with how each sample was prepared. Higher pressures of carbon dioxide during synthesis produced higher occupancies. The current samples were prepared at higher pressures (900 psi) and clearly show carbon dioxide in both cavities with the large void having a higher occupancy ( $>95\%$ ). The smaller void yielded occupancies between 60 and 80% depending on the thermal parameters. The actual amount of  $CO_2$  used in the refinement does not affect the formation and dissociation experiments significantly, so the final occupancies of 73 and 98% were calculated using the CSMHYD program provided by Sloan.<sup>1</sup> These values give large thermal parameters in comparison to the framework, but this would be expected for highly disordered atoms.

## Conclusions

In these experiments, we demonstrated that the process of formation of  $CO_2$  hydrate can be studied in situ by neutron diffraction. The rate of formation increased significantly at higher temperatures, and nearly complete conversion to the hydrate was observed when the temperature was slowly increased above the melting point of ice. In the study of the conversion of ice into  $CO_2$  hydrate, our findings support a two-stage process. The rate-limiting step of the initial stage (before a layer of hydrate covers the ice particles) is the reaction of  $CO_2$  with the QLL.<sup>35</sup> The rate of the second stage (after a layer of hydrate covers the ice particles) is controlled by the diffusion of the  $CO_2$  molecules through the layers of hydrate covering the ice particles. Our findings also suggest that after the diffusion through the hydrate layer, the  $CO_2$  forms the hydrate through a reaction with internal water in a QLL or “premelting” layer rather than with ice molecules. This opens up a large area of kinetic studies that can be done not only with the  $CO_2$  system but also with other gas hydrate systems as well. Future projects include varying the ice grain size, pressures, and the type of guest molecules.

**Acknowledgment.** The work at Argonne National Laboratory was supported by the Laboratory Directed Research and Development program and by the U.S. Department of Energy, Basic Energy Sciences—Material Sciences, under Contract W-31-109-ENG-38. We acknowledge R. Vitt and K. Volin for their help in the development and testing of the new pressure cell.

**Supporting Information Available:** Data collection parameters, atomic positions, and isotropic thermal parameters are listed. This material is available free of charge via the Internet at <http://pubs.acs.org>.

## References and Notes

- (1) Sloan, E. D. *Clathrate Hydrates of Natural Gases*, 2nd ed.; Marcel Dekker: New York, 1998.
- (2) Hammerschmidt, E. G. *Ind. Eng. Chem. Res.* **1934**, *26*, 851.
- (3) Collett, T. S. Methane Hydrate: An Unlimited Energy Resource? Presented at the International Symposium on Methane Hydrates: Resources in the Near Future? Chiba City, Japan, 1998.
- (4) Herzog, H.; Golomb, D.; Zemba, S. *Environ. Prog.* **1991**, *10*, 64.

- (5) Nishikawa, N.; Morishita, M.; Uchiyama, M.; Yamaguchi, F.; Ohtsubo, K.; Kimuro, H.; Hiraoka, R. *Energy Convers. Manage.* **1992**, *33*, 651.
- (6) Saji, A.; Yoshida, H.; Sakai, M.; Tanii, T.; Kamata, T.; Kitamura, H. *Energy Convers. Manage.* **1992**, *33*, 643.
- (7) McMullan, R. K.; Jeffrey, G. A. *J. Chem. Phys.* **1965**, *42*, 2725.
- (8) Mak, T. C.; McMullan, R. K. *J. Chem. Phys.* **1965**, *42*, 2732.
- (9) Davidson, D. W.; Ripmeester, J. A. In *Inclusion Compounds*; Davies, J. E. D., MacNichol, D. D., Eds.; Academic Press: New York, 1984; Vol. 3, Chapter 3.
- (10) Ripmeester, J. A.; Ratcliffe, C. I. *Energy Fuels* **1998**, *12*, 197.
- (11) Sloan, E. D. *Energy Fuels* **1998**, *12*, 191.
- (12) Subramanian, S.; Sloan, E. D. *Fluid Phase Equilib.* **1999**, *B13*, 158.
- (13) Koh, C. A.; Savidge, J. L.; Tang, C. C. *J. Phys. Chem. A* **1996**, *100*, 6412.
- (14) Stern, L. A.; Kirby, S. H.; Durham, W. B. *Science* **1996**, *273*, 1843.
- (15) Koh, C. A.; Soper, A. K.; Westacott, R. E.; Wisbey, R. P.; Wu, X.; Zhang, W.; Savidge, J. L. Neutron Diffraction Measurements of the nucleation and Growth Mechanisms of Methane Hydrate. Presented at the 213th National Meeting of the American Chemical Society, San Francisco, 1997.
- (16) Tse, J. S.; Handa, Y. P.; Ratcliffe, C. I.; Powell, B. M. *J. Inclusion Phenom.* **1986**, *4*, 235.
- (17) Kuhs, W. F.; Chazallon, B.; Radaelli, P.; Pauer, F.; Kipfstuhl, J. Raman spectroscopic and neutron diffraction studies on natural and synthetic clathrates of air and nitrogen. In *Proceedings of the 2nd International Conference on Natural Gas Hydrates*; PROGEP: Toulouse, France, 1996.
- (18) Ikeda, T.; Yamamuro, O.; Matsuo, T.; Mori, K.; Torii, S.; Kamiyama, T.; Izumi, F.; Ikeda, S.; Mae, S. *J. Phys. Chem. Solids* **1999**, *60*, 1527.
- (19) Kuhs, W. F.; Chazallon, B.; Klapproth, A.; Pauer, F. *Rev. High Pressure Sci. Technol.* **1998**, *7*, 1147.
- (20) Jorgensen, J. D.; Faber, J., Jr.; Carpenter, J. M.; Crawford, R. K.; Haumann, J. R.; Hitterman, R. L.; Kleb, R.; Ostrowski, G. E.; Rotella, F. J.; Worlton, T. G. *J. Appl. Crystallogr.* **1989**, *22*, 321.
- (21) Larson, A. C.; Von Dreele, R. B. *GSAS—General Structure Analysis System*; Los Alamos National Laboratory: Los Alamos, NM, 1994.
- (22) Uchida, T.; Hondoh, T.; Mae, S.; Kawabata, J. Physical Data of CO<sub>2</sub> Hydrate. In *Direct Ocean Disposal of Carbon Dioxide*; Handa, N., Ohsumi, T., Eds.; TERRAPUB: Tokyo, 1995; p 45.
- (23) Uchida, T. *Waste Manage.* **1997**, *17*, 343.
- (24) Stern, L. A.; Kirby, S. H. *Energy Fuels* **1998**, *12*, 201.
- (25) Stern, L. A.; Hogenboom, D. L.; Durham, W. B.; Kirby, S. H.; Chou, I.-M. *J. Phys. Chem. B* **1998**, *102*, 2627.
- (26) Hwang, M. J.; Wright, D. A.; Kapur, A.; Holder, G. D. *J. Inclusion Phenom. Mol. Recognit. Chem.* **1990**, *8*, 103.
- (27) Fujii, K.; Kondo, W. *J. Am. Ceram. Soc.* **1974**, *57*, 492.
- (28) FitzGerald, S. A.; Neumann, D. A.; Rush, J. J.; Bentz, D. P.; Livingston, R. A. *Chem. Mater.* **1998**, *10*, 397.
- (29) Berliner, R.; Popovici, M.; Herwig, K. W.; Berliner, M.; Jennings, H. M.; Thomas, J. J. *Cem. Concr. Res.* **1998**, *28*, 231.
- (30) Mizuno, Y.; Hanafusa, N. *J. Phys., Colloq., C1 Suppl.* **1987**, *48*, 511.
- (31) Marcus, Y.; Ben-Naim, A. *J. Phys. Chem.* **1985**, *83*, 4744.
- (32) Uchida, T.; Ebinuma, T.; Kawabata, J.; Narita, H. *J. Cryst. Growth* **1999**, *204*, 348.
- (33) Itagaki, K. *J. Phys. Soc. Jpn.* **1967**, *22*, 427.
- (34) Dash, J. G.; Fu, H. Y.; Wettlaufer, J. S. *J. Rep. Prog. Phys.* **1995**, *58*, 115.
- (35) Takeya, S.; Hondoh, T.; Uchida, T. In-Situ Observation of CO<sub>2</sub> Hydrate by X-ray Diffraction. Presented at the Third International Conference on Gas Hydrates, Salt Lake City, UT, 1999.
- (36) Furukawa, Y.; Nada, H. *J. Phys. Chem. B* **1997**, *101*, 6167.
- (37) Ocampo, J. Hydrogen bonds reorganization during clathrate hydrate growth in hexagonal ice. In *Proceedings of the NATO Advanced Research Workshop on Hydrogen Bond Networks*, Cargese, France, 1994; Kluwer Academic Publishers: Netherlands.
- (38) Ratcliffe, C. I.; Ripmeester, J. A. *J. Phys. Chem.* **1986**, *90*, 1259.
- (39) Sum, A. K.; Burruss, R. C.; Sloan, E. D. *J. Phys. Chem. B* **1997**, *101*, 7371.